

See discussions, stats, and author profiles for this publication at: <https://www.researchgate.net/publication/50349525>

# Conformations of Spermine in Adenosine Triphosphate Complex: The Structural Basis for Weak Bimolecular Interactions of Major Cellular Electrolytes

ARTICLE in CHEMISTRY - A EUROPEAN JOURNAL · APRIL 2011

Impact Factor: 5.73 · DOI: 10.1002/chem.201002759 · Source: PubMed

CITATIONS

2

READS

14

6 AUTHORS, INCLUDING:



**Keisuke Maruyoshi**

Daiichi Sankyo Company

5 PUBLICATIONS 31 CITATIONS

SEE PROFILE



**Tohru Oishi**

Kyushu University

131 PUBLICATIONS 2,366 CITATIONS

SEE PROFILE



**Michio Murata**

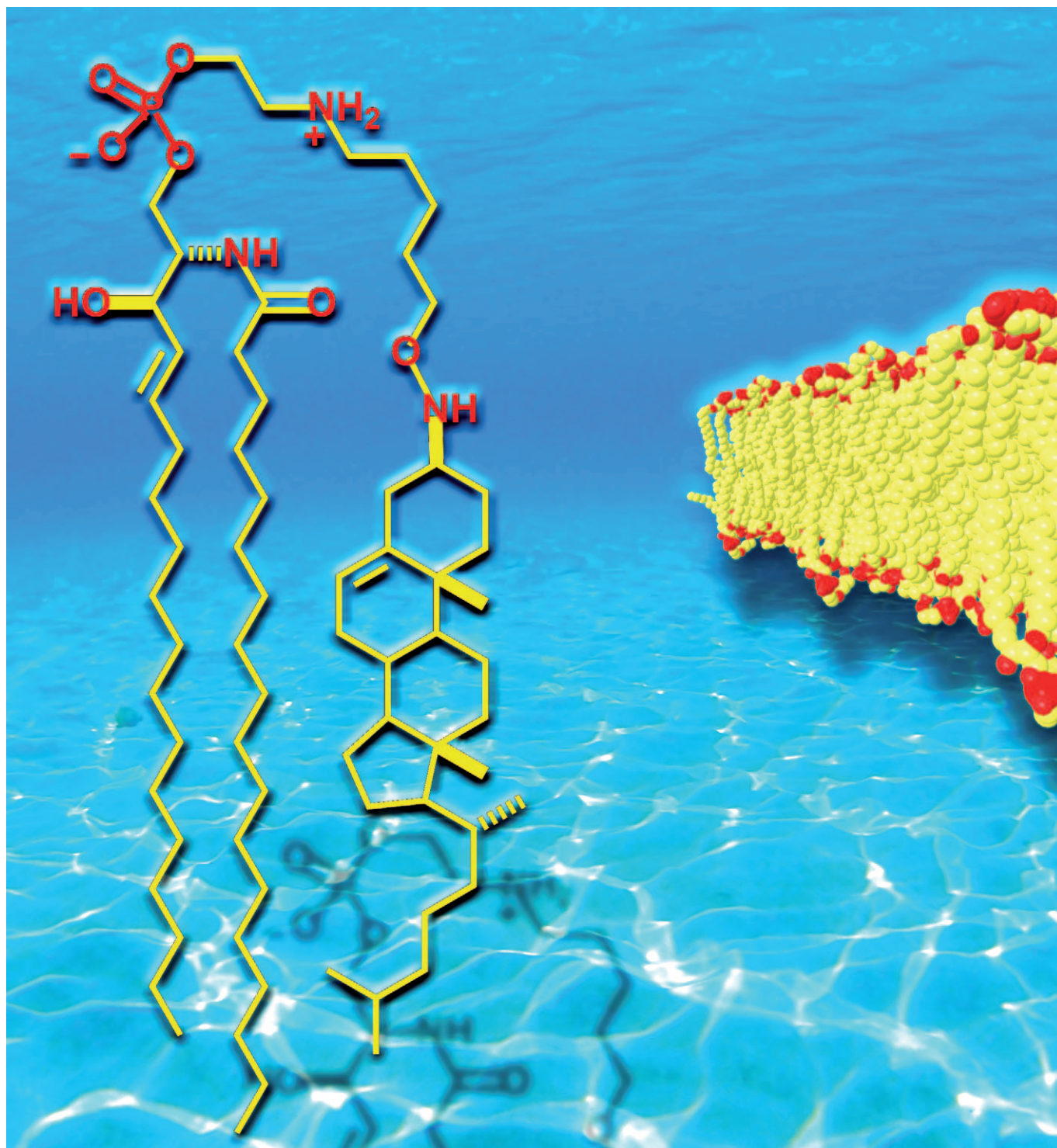
Osaka University

224 PUBLICATIONS 7,446 CITATIONS

SEE PROFILE

## Design and Synthesis of Sphingomyelin–Cholesterol Conjugates and Their Formation of Ordered Membranes

Nobuaki Matsumori,\* Norio Tanada, Kohei Nozu, Hiroki Okazaki, Tohru Oishi, and Michio Murata\*<sup>[a]</sup>



**Abstract:** A lipid raft is a cholesterol (Chol)-rich microdomain floating in a sea of lipid bilayers. Although Chol is thought to interact preferentially with sphingolipids such as sphingomyelin (SM), rather than with glycerophospholipids, the origin of the specific interaction has remained unresolved, primarily because of the high mobility of lipid molecules and weak intermolecular interactions. In this study, we synthesized SM–Chol conjugates with functionally designed linker portions to restrain Chol mobility and examined their formation of ordered membranes

by a detergent insolubility assay, fluorescence anisotropy experiments, and fluorescence-quenching assay. In all of the tests, membranes prepared from the conjugates showed properties of ordered domains comparable to a SM–Chol (1:1) membrane. To gain insight into the structure of bilayers composed from the conjugates, we performed molecular dynamics simulations with 64

molecules of the conjugates, which suggested that the conjugates form a stable bilayer structure by bending at the linker portion and, mostly, reproduce the hydrogen bonds between the SM and Chol portions. These results imply that the molecular recognition between SM and Chol in an ordered domain is essentially reproduced by the conjugated molecules and, thus, demonstrates that these conjugate molecules could potentially serve as molecular probes for understanding molecular recognition in lipid rafts.

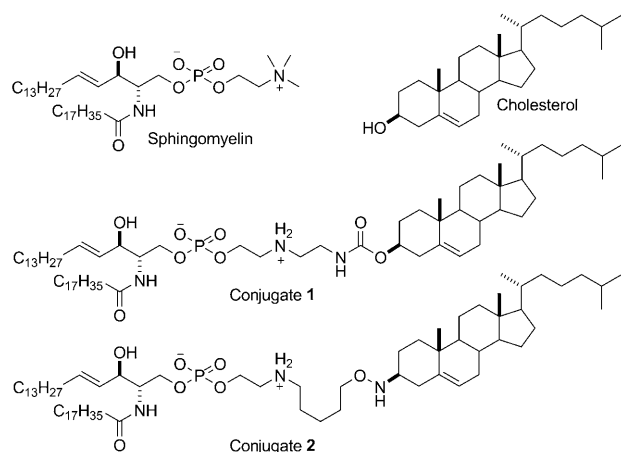
**Keywords:** cholesterol • lipids • membranes • molecular dynamics • synthesis

## Introduction

Since Simons et al. proposed the lipid rafts hypothesis in 1999,<sup>[1]</sup> formation of lipid rafts in biomembranes have attracted much attention from multidisciplinary researchers due to their potential role in signal transduction, cholesterol (Chol, Scheme 1) shuttling, and protein sorting.<sup>[2–6]</sup> Lipid rafts are microdomains, rich in saturated lipids and Chol, floating in a sea of phospholipids. The first evidence for the existence of lipid rafts was the detection of detergent-resist-

ant membrane domains that were insoluble in Triton X-100.<sup>[7]</sup> These insoluble phases were composed primarily of sphingolipids and Chol. Lipid rafts are considered to exist in an ordered liquid phase, which is characterized by tight packing but relatively high lateral mobility of lipids. Instead, unsaturated phospholipids are loosely packed and form a disordered liquid phase that is solubilized upon treatment with Triton X-100. In model membranes, Chol is able to promote the separation of ordered and disordered domains.<sup>[8–10]</sup> Therefore, the presence of Chol is generally reckoned to be one of the essential requirements for ordered-phase formation. In particular, Chol is thought to interact preferentially with sphingolipids, such as sphingomyelin (SM, Scheme 1)—a major component of lipid rafts in plasma membranes—rather than with glycerophospholipid counterparts. However, the origin of this putative specific SM–Chol interaction has not been solved in substantial detail. This is mostly attributable to the nature of the lipid rafts in that the lipid molecules are in a dissociation/association equilibrium. In other words, the interactions between lipid molecules occur transiently, which hampers experimental observations of molecular interactions in lipid bilayers at the atomic level. In fact, atom-level pictures of SM–Chol interactions and lipid-raft formation have exclusively been provided by molecular dynamics (MD) simulations.<sup>[11]</sup>

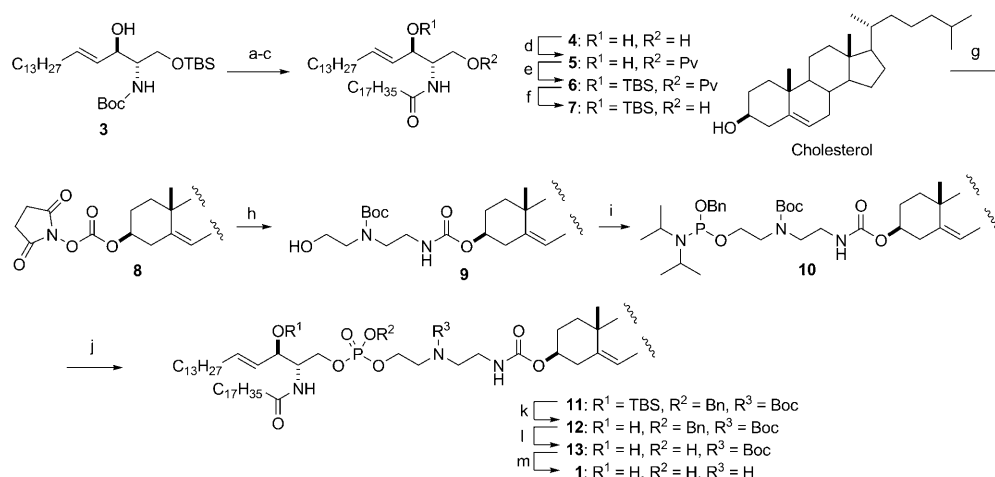
Capturing or freezing these momentary contacts to study how they interact is currently a significant goal of membrane research. In general, cross-linking with covalent bonds can provide the means for allowing transient interactions to be frozen in place or for weakly interacting molecules to be trapped in a complex stable enough for isolation and characterization. In our previous study,<sup>[12]</sup> amphotericin B—a known antibiotic that interacts with sterol molecules to form ion-channel complexes in lipid bilayers—was chemically conjugated with sterol, which led to stabilization of the interaction in membranes. Hence, in this study we covalently linked SM and Chol to stabilize the weak molecular interaction, and examined their formation of ordered membranes



Scheme 1. Structures of sphingomyelin, cholesterol, and conjugates **1** and **2**.

[a] Prof. Dr. N. Matsumori, N. Tanada, K. Nozu, H. Okazaki, Prof. Dr. T. Oishi, Prof. Dr. M. Murata  
Department of Chemistry, Osaka University  
1-1 Machikaneyama, Toyonaka  
Osaka 560-0043 (Japan)  
E-mail: matsumori@chem.sci.osaka-u.ac.jp  
murata@chem.sci.osaka-u.ac.jp

Supporting information for this article is available on the WWW under <http://dx.doi.org/10.1002/chem.201100849>.



Scheme 2. Synthesis of conjugate **1**. Reagents and conditions: a) TFA,  $CH_2Cl_2$ ,  $0^\circ C$ , 1 h; b) DMAP, 4-nitrophenyl stearate, THF, RT, 2.5 h; c) TBAF, THF,  $0^\circ C$  to RT, 30 min, 81 % (three steps); d)  $PvCl$ , pyridine,  $-10^\circ C$ , 1.5 h, 83 %; e) TBSOTf, lutidine,  $0^\circ C$ , 10 min, 93 %; f) DBU, MeOH, RT, 18 h, 78 %; g) *N,N*-disuccinimidyl carbonate,  $Et_3N$ ,  $CH_3CN$ , RT, 3 h, 93 %; h)  $H_2N(CH_2)_2NH(Boc)(CH_2)_2OH$ ,  $CH_2Cl_2$ , RT, 2 h, 90 %; i)  $(iPr)_2NP(OBn)N(iPr)_2$ , 1*H*-tetrazole,  $CH_2Cl_2$ ,  $CH_3CN$ ,  $0^\circ C$  to RT, 30 min, 85 %; j) **7**, 1*H*-tetrazole,  $CH_2Cl_2/CH_3CN$ , RT, 4 h; then *t*BuOOH,  $0^\circ C$ , 30 min, 64 %; k) TBAF, THF, RT, 1 h, 87 %; l) NaI, AcOH, acetone, RT, 3 h, 65 %; m) TFA,  $CH_2Cl_2$ ,  $0^\circ C$ , 3 h, 87 %.

by three different biophysical assays, as well as by MD simulations.

## Results and Discussion

**Design of conjugates **1** and **2**:** Recent MD simulations of lipid bilayers composed of ternary POPC/SM/Chol (POPC = 1-palmitoyl-2-oleoylphosphatidylcholine) mixtures demonstrated that a net attractive electrostatic interaction is possible between the OH group of Chol and the positively charged choline portion of SM.<sup>[13]</sup> It was explained that this charge-pair interaction between SM and Chol is stabilized by downwards bending of the SM head group due to the intramolecular hydrogen bonding of SM. Such electrostatic interaction may cause an umbrella effect, so that the choline group of SM spreads horizontally on the surface of membranes,<sup>[14]</sup> thus strongly shielding Chol from contact with the water layer. Based on this model, we first designed a conjugate molecule **1** (Scheme 1), in which the OH group of Chol and the positively charged choline portion of SM are covalently cross-linked with a carbamate. In conjugate **1**, however, the OH group of Chol was used for the carbamate formation, which results in loss of the hydrogen-bond donor at C3 of Chol. Previous experimental and simulation studies suggested that the hydroxy group of Chol interacts with the carbonyl oxygen atom of SM, as well as the choline portion of SM.<sup>[15–17]</sup> Thus, we also prepared conjugate molecule **2** (Scheme 1) to reproduce the possible hydrogen bonds formed between SM and Chol. In conjugate **2**, SM and Chol are linked by an oxyamine bond, in which the NH hydrogen atom is expected to behave as a hydrogen-bond donor. In addition, formation of the ammonium salt of the amino group in the oxyamine linkage will be suppressed due to the low basicity of the amino group.

**Synthesis of conjugates **1** and **2**:** The SM–Chol conjugates **1** and **2** could be synthesized through successive coupling of the Chol, linker, and ceramide moieties. The synthesis of conjugate **1** is illustrated in Scheme 2. The ceramide derivative **7** was synthesized from known sphingosine derivative **3**, which was prepared from L-serine by a procedure reported by Katsumura's group.<sup>[18]</sup> Removal of the *tert*-butoxycarbonyl (Boc) group of **3** with trifluoroacetic acid (TFA), followed by treatment of the resulting amine with 4-nitrophenyl stearate<sup>[19]</sup> in the presence of 4-dimethylaminopyridine (DMAP) gave the stearoyl amide. Removal of the *tert*-butyldimethylsilyl (TBS) group of the primary alcohol with tetrabutylammonium fluoride (TBAF) afforded ceramide derivative **4** in 81 % yield, over three steps. The next task was conversion of **4** to coupling precursor **7**. Because selective deprotection of the primary alcohol from the bis-TBS ether of **4** was difficult, the primary alcohol was tentatively protected as pivalate (Pv) ester **5** and the remaining secondary alcohol was converted to TBS ether **6**. Although removal of the Pv group with diisobutylaluminum hydride (DIBAL) was unsuccessful (a mixture of **7** and its silyl-migrated analogue were obtained), treatment of **6** with 1,8-diazabicyclo-[5.4.0]undec-7-ene (DBU) in MeOH, at room temperature for 18 h, afforded **7** in 78 % yield, as a single product.<sup>[20]</sup>

The Chol–linker portion of **1** was synthesized by coupling of carbonate diester **8**, prepared from Chol,<sup>[21]</sup> with *tert*-butyl-2-aminoethyl-2-hydroxyethylcarbamate to afford primary alcohol **9**. Next, the most critical issue of the present synthesis, coupling of the Chol–linker (**9**) and ceramide (**7**) moieties with a phosphodiester, was examined. An attempt to couple **9** and **7** with  $PCl_3$  was unsuccessful.<sup>[21]</sup> After several experiments, we found that the phosphoroamidite method reported by van Boom et al.<sup>[22]</sup> was suitable for this case. Thus, treatment of **9** with benzyloxy-bis(*N,N*-diisopropylami-



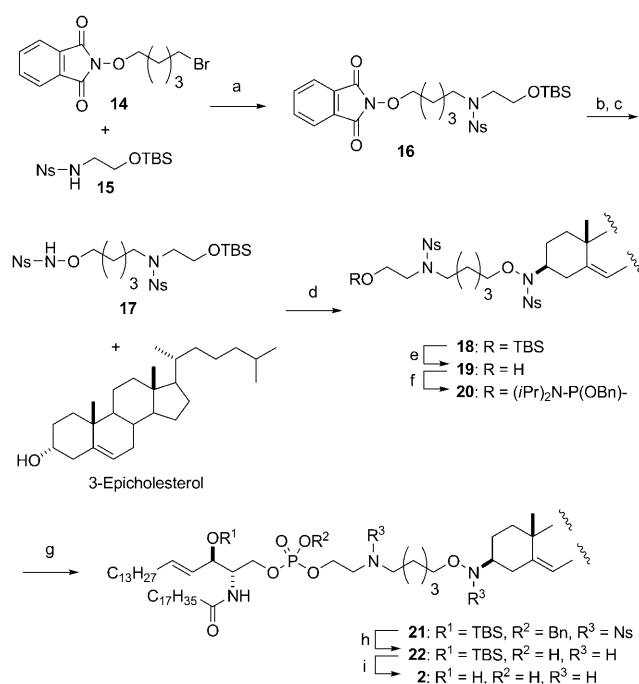
no)phosphine,<sup>[18]</sup> in the presence of 1*H*-tetrazole, resulted in the formation of amidite **10** in 85% yield. Then, treatment of **10** with **7** in the presence of 1*H*-tetrazole furnished an intermediate phosphite triester, which was oxidized with *t*BuOOH to provide phosphotriester **11** in 64% yield. The remaining task was deprotection of **11**. Removal of the TBS group with TBAF gave **12** in 87% yield. Although treatment of **12** with benzylamine to remove the benzyl (Bn) group<sup>[23,24]</sup> resulted in the formation of decomposed products, treatment with NaI in the presence of acetic acid (AcOH) afforded **13** in moderate yield (65%), with concomitant formation of decomposition products. Finally, removal of the Boc group of **13** with TFA afforded conjugate **1** in 87% yield.

Then, we synthesized conjugate **2** as shown in Scheme 3. The linker moiety **16** was prepared in 86% yield from bromide **14**<sup>[25]</sup> and nosyl (Ns)-protected amine **15** by Fukuyama coupling<sup>[26]</sup> in the presence of K<sub>2</sub>CO<sub>3</sub> in DMSO at 65°C for 5 h. Removal of the phthalimide group of **16** with hydrazine, followed by introduction of a Ns group by treatment with NsCl in the presence of Et<sub>3</sub>N, yielded amide **17**. Coupling of **17** and 3-epicholesterol,<sup>[27]</sup> prepared by oxidation of Chol with pyridinium chlorochromate (PCC) and subsequent stereoselective reduction with L-Selectride, was achieved by the Fukuyama–Mitsunobu reaction.<sup>[26]</sup> Treatment of **17** and 3-epicholesterol with diethyl azodicarboxylate (DEAD) in

the presence of Ph<sub>3</sub>P resulted in the formation of coupling compound **18** in 38% yield and concomitant dehydration of 3-epicholesterol. Removal of the TBS group of **18** gave alcohol **19**, which was converted to phosphotriester **21** (59%) via amidite **20** (96%) in an analogous sequence to that described in Scheme 2. In contrast to conjugate **1**, the final deprotection steps were problematic. Although the TBS and Bn groups of **21** were removed under the earlier conditions (Scheme 2, steps k and l), removal of the Ns groups did not proceed at all. To see whether the Ns group of **21** was removable, **21** was treated with PhSH in the presence of K<sub>2</sub>CO<sub>3</sub> in DMF, at 0°C to room temperature for 4 h. Unexpectedly, not only removal of the Ns groups, but also concomitant removal of the Bn group, occurred to give **22**. Although treatment of **22** with TBAF gave a complex mixture, treatment with HF·pyridine (Py) afforded conjugate **2** in 11% yield from **21**. The low yield of **2** was partially due to losses during purification by HPLC.

### Detergent insolubility of membranes formed from conjugates **1** and **2**:

With **1** and **2** available, we next examined the level of ordered-domain formation of membranes comprised of these conjugates by using a detergent insolubility assay.<sup>[8,28–31]</sup> In this method, the light scattering by multilamellar vesicles was recorded as optical density (OD). The percentage OD (% OD) remaining after addition of Triton X-100 to the vesicle suspension roughly corresponds to the fraction of detergent-resistant membranes.<sup>[28]</sup> Throughout this study, we used 18:0 SM purified by HPLC from a bovine brain SM mixture because commercially available semisynthetic 18:0 SM turned out to be a mixture of epimers at C3 of sphingosine. Liposomes composed of SM, a 1:1 mixture of SM/Chol, and conjugates **1** and **2** were subjected to this assay. Although the pure 18:0 SM membrane is almost solubilized by Triton X-100, the addition of Chol to the SM liposomes markedly decreased the solubility as seen from the increased % OD values (Table 1). Notably,



Scheme 3. Synthesis of conjugate **2**. Reagents and conditions: a) NsNH-(CH<sub>2</sub>)<sub>2</sub>OTBS, **15**, K<sub>2</sub>CO<sub>3</sub>, DMSO, 65°C, 5 h, 86%; b) N<sub>2</sub>H<sub>4</sub>·H<sub>2</sub>O, EtOH, RT, 4 h; c) NsCl, Et<sub>3</sub>N, CH<sub>2</sub>Cl<sub>2</sub>/MeOH (1:1), 0°C to RT, 2 h, 30% (two steps); d) Ph<sub>3</sub>P, DEAD, toluene/THF (3:1), 0°C to RT, 1 h, 38%; e) TBAF, THF, 0°C to RT, 1 h, 88%; f) (iPr)<sub>2</sub>NP(OBn)N(iPr)<sub>2</sub>, 1*H*-tetrazole, CH<sub>2</sub>Cl<sub>2</sub>, CH<sub>3</sub>CN, 0°C to RT, 1 h, 96%; g) **3**, 1*H*-tetrazole, CH<sub>2</sub>Cl<sub>2</sub>/CH<sub>3</sub>CN, RT 1 h; then *t*BuOOH, 0°C, 30 min, 59%; h) PhSH, DMF, K<sub>2</sub>CO<sub>3</sub>, 0°C to RT, 4 h; i) HF·Py, THF, 0°C to 55°C, 1.5 h, 11% (two steps).

Table 1. Detergent insolubility of multilamellar vesicles.<sup>[a]</sup>

	Membrane composition			
	SM	SM/Chol	Conjugate <b>1</b>	Conjugate <b>2</b>
% OD <sup>[b]</sup>	2.5	94.5	94.2	93.1

[a] Multilamellar vesicles were composed of SM, SM/Chol (1:1), or conjugates **1** or **2**. [b] % OD represents the optical density that remained after incubation of the vesicles in the presence of Triton X-100 (0.5%). Values represent averages, *n* = 3.

the membranes formed by conjugates **1** and **2** were tolerant to Triton X-100 to similar extents to the SM/Chol membrane (Table 1). These results demonstrate that both conjugates can form Triton-resistant membranes, thereby suggesting that both **1** and **2** also form ordered-membrane domains.

### Fluorescence-quenching assay for evaluating domain formation:

Fluorescence-quenching experiments were carried out to further evaluate the domain formation of conjugates **1** and **2**. In this method, quenching of the fluorescence of

membrane-inserted 1,6-diphenyl-1,3,5-hexatriene (DPH) is measured in model membrane vesicles that contain fluorescence-quenching phospholipid 1-palmitoyl-2(12-doxyl)stearoylphosphatidylcholine (12SLPC), which has phase behavior similar to that of a lipid with unsaturated acyl chains, such as dioleoylphosphatidylcholine (DOPC).<sup>[8,10,28,32–34]</sup> Formation of ordered domains rescues DPH molecules that reside in the domains from quenching. Upon domain formation of a SM/Chol system, DPH fluorescence intensity ( $F$ ) is obtained from vesicles composed of DPH, SM, Chol, and 12SLPC. The fractional quenching in such mixtures is given by the DPH fluorescence intensity ( $F$ ) normalized to that obtained from vesicles composed of DPH, SM, Chol, and DOPC ( $F_0$ ), in which the quencher lipid 12SLPC is replaced by the unlabeled analogue DOPC. When domain formation occurs in a mixed lipid bilayer that contains 12SLPC, the domain formation results in reduced quenching of DPH relative to a homogeneously mixed bilayer that contains 12SLPC. The degree of domain formation is related to  $\Delta F/F_0$ —the difference between the fraction of DPH fluorescence that is unquenched in a sample containing SM-rich domains and the fraction of unquenched fluorescence in a sample having the same amount of quencher lipid but lacking such domains.<sup>[28]</sup> To evaluate domain formation of the conjugates in this assay, the SM/Chol mixture was replaced by each conjugate. Figure 1 shows  $\Delta F/F_0$  values of a SM/

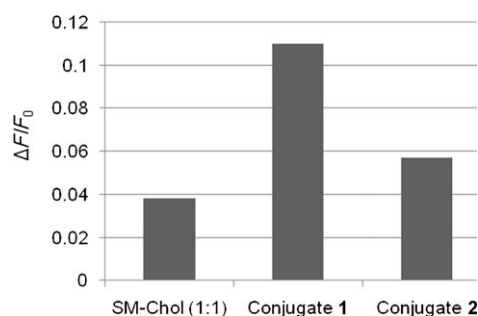


Figure 1. Domain formation of SM/Chol (1:1) and conjugates **1** and **2** evaluated by fluorescence-quenching experiments.  $\Delta F/F_0$  at 23°C in SM/Chol/12SLPC and conjugate/12SLPC mixtures.

Chol mixture (1:1) and conjugates **1** and **2** at 23°C; both conjugates gave larger  $\Delta F/F_0$  values than the SM/Chol mixture. Notably, the  $\Delta F/F_0$  values can be affected, not only by the degree of domain formation, but also by domain size;<sup>[28]</sup> larger domains tend to give rise to larger  $\Delta F/F_0$  values. Therefore, the observed larger  $\Delta F/F_0$  values for the conjugates do not necessarily mean a higher degree of domain formation, but may suggest formation of larger domains. In any case, both conjugates **1** and **2** seem to form stable raft-like domains.

**Fluorescence anisotropy assay for evaluating domain formation:** To further examine how the conjugates form highly ordered membranes, we measured the steady-state fluorescence anisotropy of DPH in vesicles formed by **1** and **2** com-

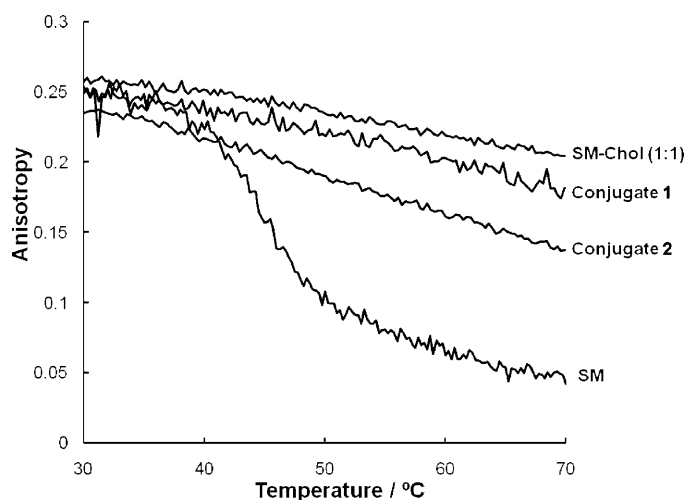


Figure 2. Fluorescence anisotropy of DPH in membranes composed of SM, SM/Chol (1:1), **1**, and **2** measured as a function of temperature. The total lipid concentration (phospholipids and sterol) was 53.3  $\mu\text{M}$  and the DPH/lipids molar ratio was 1:50.

pared with SM and 1:1 SM/Chol vesicles (Figure 2). The higher the DPH fluorescence anisotropy becomes, the more tightly the lipids are packed (ordered).<sup>[30]</sup> The SM membrane showed the phase-transition at around 45°C (Figure 2), whereas the SM/Chol membrane lacked an apparent phase-transition temperature and the anisotropy dramatically increased across the temperature range. The membranes formed by conjugates **1** and **2** did not exhibit an explicit phase-transition temperature and, again, showed relatively high anisotropy for the whole measurable temperature range, which supports the formation of ordered membranes by these conjugates. However, compared with the SM/Chol (1:1) membrane, smaller fluorescent anisotropy of both conjugates **1** and **2** may suggest the formation of less-ordered phases. As in the aforementioned fluorescence-quenching experiments, conjugate **1** showed higher anisotropy relative to conjugate **2**.

**Atomic-scale molecular dynamics simulations:** The aforementioned assays grossly suggest that conjugates **1** and **2** form ordered membranes with properties similar to the ordered domains formed by SM/Chol, although fluorescence anisotropy experiments (Figure 2) indicate that membranes formed by conjugates **1** and **2** are both slightly less ordered relative to the SM/Chol (1:1) membrane. When comparing conjugates **1** and **2** in ordered membrane formation (Figures 1 and 2), we could not find superiority of conjugate **2**, which was originally designed to better reproduce the intermolecular hydrogen bonds between SM and Chol. Hence, to better understand the membrane structures formed by the conjugates, as well as the difference in domain formation properties among **1**, **2**, and SM/Chol (1:1) membranes, we performed atomic-scale MD simulations.

Figure 3 shows a snapshot of the MD simulation for the bilayer system of 64 molecules of conjugate **2**, which forms a

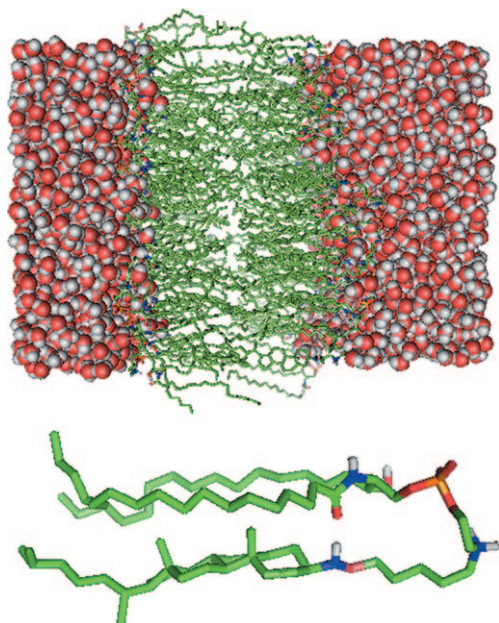
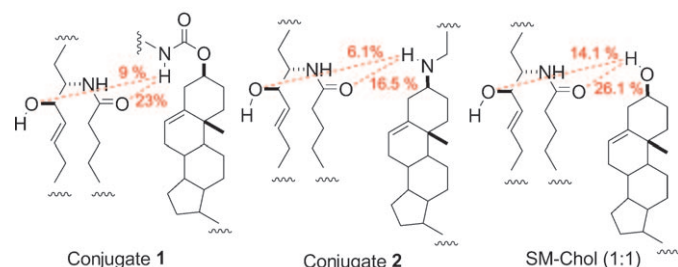


Figure 3. Top: Snapshot of the MD simulation for the bilayer system of conjugate **2** surrounded by water. Conjugate molecules are shown in green, and water molecules are depicted by space-filling models. Bottom: A representative snapshot of conjugate **2** in the bilayers.

stable bilayer structure. Each conjugate molecule bends at the linker portion, which reproduces the normal orientation of lipids in the bilayers. Conjugate **1** also forms similar bilayers by bending at its linker portion. Thus, the membrane formation of conjugates **1** and **2** was confirmed both experimentally and theoretically.

We next discuss the intermolecular interactions responsible for the increased order of the conjugate **1** membrane relative to that of conjugate **2**. As mentioned above, we were concerned that the carbamate linkage of conjugate **1** would change the nature of the hydrogen bonding with Chol, which prompted us to design conjugate **2** with the alkoxyamine linkage. However, the fluorescence anisotropy experiments (Figure 2) suggested that conjugate **1** constitutes the ordered phase more effectively than **2**. This unexpected result may be explained by the hydrogen bonds formed by the carbamate linker of conjugate **1** (Scheme 4), which func-



Scheme 4. Predominant hydrogen bonds deduced from MD simulations for membranes composed of **1**, **2**, and SM/Chol (1:1). Values in red represent the calculated average hydrogen bond.

tions as hydrogen-bond donor more efficiently than the oxy-amino group in conjugate **2**. The stronger hydrogen bonds formed with the carbamate group of **1** can mimic the SM–Chol interactions necessary for ordered-phase formation and, thereby, result in more effective domain formation in conjugate **1**. This explanation holds true for the fact that the SM/Chol (1:1) system showed higher domain formation than the membranes formed by conjugate molecules (Scheme 4).

## Conclusion

We have prepared SM–Chol conjugated molecules **1** and **2** by chemical synthesis and evaluated their domain formation by detergent insolubility, fluorescence anisotropy, and fluorescence-quenching experiments. All assays suggested that both conjugates **1** and **2** form ordered membranes with properties similar to the SM/Chol system, although conjugate **1** showed superior domain-formation properties relative to **2**. The MD simulations also suggested that the conjugates form stable bilayers by bending at the linker portion and, mostly, reproduce the hydrogen bonds between the SM and Chol portions. Particularly, **1** showed higher hydrogen-bond formation than **2**, mainly due to the carbamate moiety that acts as a hydrogen-bond donor. This is consistent with the finding that domain formation in **1** is more effective than in **2**. Finally, this study suggests that putative SM–Chol interactions in lipid rafts can be reproduced by these conjugated molecules to a considerable extent and, therefore, demonstrates that, after some improvements in their molecular design, SM–Chol conjugates could serve as a powerful tool for the study of intermolecular recognition in lipid rafts.

## Experimental Section

Experimental details for the synthesis of conjugates **1** and **2** are reported in the Supporting Information.

**General information for assays:** DOPC, 12SLP, and bovine brain SM were purchased from Avanti Polar Lipids (Alabaster, AL). Chol and Triton X-100 were purchased from Nacalai Tesque (Kyoto, Japan). DPH was purchased from Aldrich (St. Louis, MO). 18–0 SM was purified by HPLC from bovine brain SM. Voltex mixers VOLTEX-GENIE (Scientific Industries) and ultrasonic cleaner BRANSON 1510 (Yamato Inc.) were used for liposome preparation.

### Percent solubilization experiments

**Sample preparation for solubility experiments:** A solution of SM (500 nmol), 1:1 SM–Chol (total 500 nmol), conjugate **1** or **2** (250 nmol) in 1:1 MeOH/CHCl<sub>3</sub> was dried under a stream of nitrogen, redissolved in chloroform, then dried again under a stream of nitrogen. After the lipids were further dried under high vacuum for at least 12 h, they were hydrated (swelled) by addition of pH 7 phosphate buffered saline (PBS buffer, 0.95 mL). To uniformly disperse the lipids and form homogeneous multilamellar lipid vesicles, each sample was vigorously vortexed at 65°C, well above the phase-transition temperature of SM, then cooled to RT.

**Measurement of solubilization by the loss of light scattering:** The optical density of the samples was measured at 400 nm on a Shimadzu UV-2500 spectrophotometer. Triton X-100/PBS buffer (10% (w/v), 50 µL) was added. After mixing and incubation at 23°C for 2 h, the optical density was remeasured. The ratio of optical density after Triton X-100 incuba-

tion (not corrected for dilution with Triton X-100 solution) to that before the addition of Triton X-100 (%OD) was then calculated.

**Fluorescence quenching experiments:** By the procedure described above, the following multilamellar vesicles (50 nmol total lipids) were prepared in PBS buffer (pH 7, 1 mL): SM/Chol/12SLPC (1:1:1) containing 1% DPH ( $F$  sample); SM/Chol/12SLPC (1:1:1) ( $F_b$  sample); DOPC/Chol/12SLPC (1:1:1) containing 1% DPH ( $F_c$  sample); DOPC/Chol/12SLPC (1:1:1) ( $F_{bc}$  sample); SM/Chol/DOPC (1:1:1) containing 1% DPH ( $F_0$  sample); SM/Chol/DOPC (1:1:1) ( $F_{0b}$  sample); DOPC/Chol (2:1) containing 1% DPH ( $F_{0c}$  sample); DOPC/Chol (2:1) ( $F_{0bc}$  sample). To evaluate domain formation of the conjugates in this assay, 1:1 SM-Chol mixture was replaced by each conjugate. Fluorescence was measured on a JASCO FP-6600 spectrofluorometer at RT with a 1 cm excitation, 4 mm emission path length quartz cuvette. The excitation/emission wavelength settings were 359 and 427 nm, respectively. Excitation and emission slits with a band pass of 1 and 6 nm, respectively, were used for all measurements.  $\Delta F/F_0$  values were calculated by inputting the fluorescence intensities into the following equation:  $\Delta F/F_0 = (F - F_b)/(F_0 - F_{0b}) - (F_c - F_{bc})/(F_{0c} - F_{0bc})$ .

**Fluorescence anisotropy measurements:** Multilamellar vesicles of lipids containing DPH (2 mol%) were prepared by drying a solution of SM (160 nmol), 1:1 SM-Chol (total 160 nmol), conjugate **1** or **2** (80 nmol) and DPH (3.2 nmol) in 1:1 MeOH/CHCl<sub>3</sub> under a stream of argon, redissolving the residue in CHCl<sub>3</sub>, and drying under a stream of argon. After the lipids were further dried under high vacuum for at least 12 h, they were hydrated (swelled) by addition of PBS buffer (pH 7.0, 3 mL). To uniformly disperse the lipids and form homogeneous multilamellar lipid vesicles, each sample was vigorously vortexed at 65 °C, well above the phase-transition temperature of SM, and then cooled to RT. The samples were subjected to three freeze-thaw cycles in liquid nitrogen and a water bath maintained at 65 °C. Fluorescence polarization measurements were performed with a JASCO FP-6600 spectrofluorometer equipped with a JASCO ADP-303 polarization accessory. Quartz cuvettes with a path length of 1 cm were used. The excitation wavelength was set at 358 nm and emission was monitored at 430 nm. Excitation and emission slits with a band pass of 1 and 10 nm, respectively, were used for all measurements. The excitation slit used was the smallest possible to minimize any photoisomerization of DPH during irradiation. The measurement temperature was raised from 30 to 70 °C with a 2 °C min<sup>-1</sup> gradient, and fluorescence was measured with a 2 s response. Polarization values were calculated with Spectra Manager software attached to the spectrofluorometer.

**Atomic-scale simulation:** We studied three bilayers composed of: 1) 64 SM and 64 Chol units, 2) 64 molecules of **1**, and 3) 64 molecules of **2**. The initial structure of the membrane comprised of 64 SM and 64 Chol units was built by modification of the membrane composed of 128 SM and 3655 water molecules, reported by Niemelä et al.,<sup>[35]</sup> 64 SM molecules were chosen from 128 SM molecules of the membrane and replaced by 64 Chol molecules. The same number of SM molecules were replaced in each leaflet and the structure of the bilayer was energy minimized. Force-field parameters for the SM and Chol molecules were taken from references [35,36], respectively. The initial structure of Chol was also taken from reference [36]. The initial structures of the membranes composed from conjugates **1** and **2** were built as follows: the molecular structures of the conjugates were generated by Dundee PRODRG Server,<sup>[37]</sup> then the Chol parts were replaced by the reported structure.<sup>[36]</sup> A leaflet was formed by distributing 32 molecules on the  $x,y$  plane to avoid van der Waals contacts. The second layer was obtained from the first by 180° rotation. The obtained bilayer was hydrated with 3655 simple point charge water molecules and energy minimization was performed to give the initial membrane structure. Force-field parameters for conjugate molecules were constructed in three parts for SM, the linker, and Chol. For the SM unit, the bonded and nonbonded parameters were taken from reference [35], expect that the parameters of ammonium were adopted from GROMOS force field (ff43Ga1.itp). For the linker, the bonded parameters were taken from GROMOS force field (ff43Ga1.itp) but the bonded parameters for the -O-NH- structure were adopted from the parameters generated by using the Dundee PRODRG Server. The partial charge for the -O-NH- structure was calculated at the HF/6-31G

level. The force-field parameters for the Chol portion were taken from reference [36]. For all simulations and energy minimizations GROMACS (Ver. 3.3.1) modeling software was used. All lipids and Chol bond lengths were constrained with the LINCS algorithm,<sup>[38]</sup> whereas the SETTLE algorithm<sup>[39]</sup> was used for water. The simulations were performed in the constant NPT (the number of molecules, the pressure, and the temperature) ensemble with semi-isotropic pressure coupling. The time step was set to 2.0 fs. Each simulation covered a time scale of 10.0 ns, which included an equilibration period of 8.0 ns prior to the analysis step. The treatment of long-range interactions were handled by using the particle-mesh Ewald technique.<sup>[40]</sup> A 1.0 nm cutoff in the direct space and 0.15 nm Fourier spacing were used. For the van der Waals interactions, a twin range cut-off (1.0/1.6 nm) was applied. The neighbor-pair list was updated every five steps. Temperature boundary conditions were set by using the Nose-Hoover thermostat<sup>[41]</sup> with a time constant ( $\tau$ ) = 0.1 ps. Pressure-boundary conditions were set with the Parrinello-Rahman barostat,<sup>[42]</sup>  $\tau$  = 1.0 ps. The reference temperature was  $T$  = 323 K, which is above the main phase-transition temperature of 18:0 SM.

## Acknowledgements

We are grateful to Dr. Jun Shimokawa and Prof. Tohru Fukuyama (The University of Tokyo) for helpful discussion on the nosyl chemistry. This work was supported by Grant-In-Aids for Scientific Research (B) (No. 20310132) and (S) (No. 18101010) from MEXT, Japan.

- [1] K. Simons, E. Ikonen, *Nature* **1997**, *387*, 569–572.
- [2] R. G. W. Anderson, K. Jacobson, *Science* **2002**, *296*, 1821–1825.
- [3] W. H. Binder, V. Barragan, F. M. Menger, *Angew. Chem.* **2003**, *115*, 5980–6007; *Angew. Chem. Int. Ed.* **2003**, *42*, 5802–5827.
- [4] K. Simons, D. Toomre, *Nat. Rev. Mol. Cell Biol.* **2000**, *1*, 31–39.
- [5] E. Ikonen, *Curr. Opin. Cell Biol.* **2001**, *13*, 470–477.
- [6] D. A. Brown, E. London, *Annu. Rev. Cell Dev. Biol.* **1998**, *14*, 111–136.
- [7] D. A. Brown, E. London, *Biochem. Biophys. Res. Commun.* **1997**, *240*, 1–7.
- [8] S. N. Ahmed, D. A. Brown, E. London, *Biochemistry* **1997**, *36*, 10944–10953.
- [9] T. Baumgart, S. T. Hess, W. W. Webb, *Nature* **2003**, *425*, 821–824.
- [10] J. R. Silvius, D. del Giudice, M. Lafleur, *Biochemistry* **1996**, *35*, 15198–15208.
- [11] For a recent review, see P. S. Niemelä, M. T. Hyvönen, I. Vattulainen, *Biochim. Biophys. Acta Biomembr.* **2009**, *1788*, 122–135.
- [12] a) N. Matsumori, N. Eiraku, S. Matsuoka, T. Oishi, M. Murata, T. Aoki, T. Ide, *Chem. Biol.* **2004**, *11*, 673–679; b) Y. Kasai, N. Matsumori, Y. Umegawa, S. Matsuoka, H. Ueno, H. Ikeuchi, T. Oishi, M. Murata, *Chem. Eur. J.* **2008**, *14*, 1178–1185.
- [13] J. Aittoniemi, P. S. Niemelä, M. T. Hyvönen, M. Karttunen, I. Vattulainen, *Biophys. J.* **2007**, *92*, 1125–1137.
- [14] J. Huang, G. W. Feigenson, *Biophys. J.* **1999**, *76*, 2142–2157.
- [15] G. A. Khelashvili, H. L. Scott, *J. Chem. Phys.* **2004**, *120*, 9841–9847.
- [16] T. Rog, M. Pasenkiewicz-Gierula, *Biophys. J.* **2006**, *91*, 3756–3767.
- [17] M. P. Veiga, J. L. R. Arrondo, F. M. Goni, A. Alonso, D. Marsh, *Biochemistry* **2001**, *40*, 2614–2622.
- [18] T. Yamamoto, H. Hasegawa, T. Hakogi, S. Katsumura, *Org. Lett.* **2006**, *8*, 5569–5572.
- [19] P. Shenbagamurthi, B. Kundu, J. M. Becker, P. Naider, *Int. J. Peptide Protein Res.* **1985**, *25*, 187–196.
- [20] P. Zimmermann, R. R. Schmidt, *Liebigs Ann. Chem.* **1988**, 663–667.
- [21] M. Uragami, N. Tokutake, X. Yan, S. L. Regen, *J. Am. Chem. Soc.* **2001**, *123*, 5124–5125.
- [22] C. E. Dreef, C. J. J. Elie, P. Hoogerhout, G. A. van der Marel, J. H. van Boom, *Tetrahedron Lett.* **1988**, *29*, 6513–6516.
- [23] M. D. M. Gray, D. J. H. Smith, *Tetrahedron Lett.* **1980**, *21*, 859–860.
- [24] C. J. J. Elie, C. E. Dreef, R. Verduyn, G. A. Van Der Marel, J. H. van Boom, *Tetrahedron* **1989**, *45*, 3477–3486.



- [25] R. Yoda, Y. Matsushima, *Chem. Pharm. Bull.* **1994**, *42*, 1935–1937.
- [26] T. Fukuyama, C.-K. Jow, M. Cheung, *Tetrahedron Lett.* **1995**, *36*, 6373–6374.
- [27] S. Boonyarattanakalin, S. E. Martin, S. A. Dykstra, R. Blake, B. R. Peterson, *J. Am. Chem. Soc.* **2004**, *126*, 16379–16386.
- [28] X. Xu, E. London, *Biochemistry* **2000**, *39*, 843–849.
- [29] X. Xu, R. Bittman, G. Duportail, D. Heissler, C. Vilcheze, E. London, *J. Biol. Chem.* **2001**, *276*, 33540–33546.
- [30] A. Arora, H. Raghuraman, A. Chattopadhyay, *Biochem. Biophys. Res. Commun.* **2004**, *318*, 920–926.
- [31] J. B. Massey, H. J. Pownall, *Biochemistry* **2005**, *44*, 10423–10433.
- [32] E. London, G. W. Feigenson, *Biochim. Biophys. Acta Biomembr.* **1981**, *649*, 89–97.
- [33] E. London, D. A. Brown, X. Xu, *Methods Enzymol.* **2000**, *312*, 272–290.
- [34] S. Vainio, M. Jansen, M. Koivusalo, T. Róg, M. Karttunen, I. Vattulainen, E. Ikonen, *J. Biol. Chem.* **2006**, *281*, 348–355.
- [35] P. S. Niemelä, M. T. Hyvonen, I. Vattulainen, *Biophys. J.* **2004**, *87*, 2976–2989.
- [36] M. Höltje, T. Förster, B. Brandt, T. Engels, W. V. Rybinski, H.-D. Höltje, *Biochim. Biophys. Acta Biomembr.* **2001**, *1511*, 156–167.
- [37] <http://davapc1.bioch.dundee.ac.uk/prodrg/index.html>.
- [38] B. Hess, H. Bekker, H. J. C. Berendsen, G. E. M. Fraaije, *J. Comput. Chem.* **1997**, *18*, 1463–1472.
- [39] S. Miyamoto, S. Kollman, *J. Comput. Chem.* **1992**, *13*, 952–962.
- [40] U. Essmann, L. Perera, M. L. Berkowits, H. L. T. Darden, L. G. Pedersen, *J. Chem. Phys.* **1995**, *103*, 8577–8592.
- [41] S. Nosé, *Mol. Phys.* **1984**, *52*, 255–268.
- [42] M. Parrinello, A. Rahman, *J. Appl. Phys.* **1981**, *52*, 7182–7190.

Received: March 19, 2011  
Published online: July 4, 2011